PAPER

Effects of non-isothermal flow on groundwater recharge in a semi-arid region

Zaiyong Zhang [1,2] · Wenke Wang [1,2] · Chengcheng Gong [1,2] · Ming Zhao [1,2] · Zhoufeng Wang [1,2] · Haizhen Ma [1,2]

Abstract

Groundwater recharge is critical to water circulation in arid and semi-arid regions. The accurate determination of groundwater recharge is required for assessing water resources and effectively managing groundwater, especially in water-limited areas. Based on field experiments and numerical models in a semi-arid region, this study assessed the effect of non-isothermal flow on groundwater recharge. A lysimeter was used in the Mu Us Desert, northwestern China, to monitor groundwater recharge from 1 June to 30 September 2018. The numerical models (isothermal and non-isothermal models) were calibrated with the measured soil moisture and soil temperature. Groundwater recharge was found to take up nearly 29% of rainfall. The non-isothermal model was capable of accurately assessing groundwater recharge based on the accurate calculation of evaporation. The isothermal model, however, underestimated the groundwater recharge by 13.2% and overestimated the evaporation by 16.2%. The isothermal model overestimated evaporation during the drying process. In contrast, cumulative net recharge was underestimated after heavy rainfall events. It was therefore suggested that the non-isothermal flux should be considered in semi-arid regions, especially when assessing groundwater recharge.

Keywords Groundwater recharge · China · Numerical modeling · Unsaturated zone

Introduction

Groundwater is a vital source of fresh water worldwide (Varis 2014). Globally, over 1.5 billion people use groundwater as a source of potable water (Sakram and Adimalla 2018). As the world's population continues rising, more people will rely on groundwater, especially in arid and semi-arid regions (Hamed 2013). To ensure that the groundwater supply for emerging populations is available in the long term, it is necessary to develop and implement an effective management plan. Accordingly, the determination of groundwater recharge is

critical in order to achieve efficient groundwater management (Gleeson et al. 2016). Accurately assessing groundwater recharge remains challenging, however, continues to be a hot research topic in hydrological science (Camacho Suarez et al. 2015) since recharge is difficult to measure directly and varies extensively in space and time.

The assessment of groundwater recharge in arid and semi-arid regions is more difficult in the relatively deep unsaturated zone and in complex climatic conditions (Li et al. 2017). Thus far, numerous methods have been proposed in attempts to determine groundwater recharge from available climatic and hydrogeologic observations (Meixner et al. 2016; Hartmann et al. 2017; Bhaskar et al. 2018; Zhao et al. 2020). Based on data-gathering techniques, the methods for estimating groundwater recharge can be categorized in terms of the following (Xu and Beekman 2019): (1) data from surface-related approaches such as remote sensing techniques, land-use change, and evapotranspiration; (2) data from subsurface approaches, including vadose zone methods, methods based on groundwater level data (Nimmo et al. 2015; Cuthbert et al. 2016), and tracer methods (Moeck et al. 2017; Huang et al. 2017); and (3) data related to conceptual approaches such as numerical models and water budget methods.

✉ Wenke Wang
wenkew@chd.edu.cn

1   Key Laboratory of Subsurface Hydrology and Ecological Effects in Arid Region, Chang'an University, Ministry of Education, Xi'an, The People's Republic of China

2   School of Water and Environment, Chang'an University, Yanta Road 126, 710054 Xi'an, Shaanxi, The People's Republic of China

A wide range of lysimeters have been adapted to capture the groundwater recharge within a prescribed area (Meissner et al. 2010). Lysimeters may be either non-weighing or weighing (Meshkat et al. 1999). Water gains and losses in weighing lysimeters are quantified by weighing the entire lysimeter. In non-weighing lysimeters, water fluxes are either estimated from observations of soil moisture content, or measured by volume after the water has drained or been extracted from the soil (Bergström 1990). Numerical models based on Richards' equation, involving HYDRUS (Tonkul et al. 2019), VS2DI (Szymkiewicz et al. 2015), SHAW (Gosselin et al. 2016), SWAT (Jin et al. 2015), and SWIM (Purandara et al. 2018) methods, have been utilized to assess groundwater recharge. Numerical modeling can efficiently investigate different hypothetical scenarios. Moreover, it can be adopted to simulate future groundwater recharge if the model is calibrated and validated rigorously. Turkeltaub et al. (2015) developed into the calibration of a Richards' equation-based model with transient deep vadose zone data. They reported that recharge fluxes are largely affected by the relatively recent precipitation patterns. Lu et al. (2011) studied five representative sites in order to ascertain the effects of irrigation and water table depth on groundwater recharge using a numerical model. They highlighted that different time lags corresponding to different water table depths should be considered when assessing groundwater recharge. Batalha et al. (2018) employed the HYDRUS-1D method to assess the sensitivity of groundwater recharge to the use of meteorological time series of different temporal resolutions. As revealed by their results, an increase in the time over which the meteorological data were averaged led to a lower assessment of groundwater recharge. Most groundwater recharge studies, however, have utilized isothermal models, thereby overlooking the effects of temperature. The application of the aforementioned methods of assessing groundwater recharge in arid and semi-arid regions is subject to various challenges, primarily due to the large diurnal temperature ranges in these areas, as well as the fact that precipitation events occur in short pulses, with highly variable intensities. Wang et al. (2011) demonstrated that if the higher temperature of the soil–atmosphere interface is overlooked in arid and semi-arid regions, this will cause larger errors in the isothermal modeling of the flux between the water table and the atmosphere.

Although it is widely recognized that water and heat transport should be coupled in order to determine the processes of groundwater recharge and discharge (Ren et al. 2017a), the non-isothermal model remains limited in most practical applications since it is complex and requires more observed data in order to calibrate parameters. Hou et al. (2016) constructed a HYDRUS-1D model to simulate the coupling of water, vapor, and heat in desert soil. Subsequently, the calibrated model was adopted to assess groundwater recharge. They found that the assessed groundwater recharge rates were significantly higher

than those based on chemical information. Ren et al. (2017a) tested the coupling of water and heat transport in the root zone of winter wheat and found the non-isothermal model to be highly accurate in simulating soil moisture and temperature variations. Ren et al. (2017b) ascertained the effects of temperature gradient on soil-water–salt transfer with evaporation in the laboratory. They reported that the non-isothermal model could achieve better results than the isothermal model since the effect of temperature gradient on salt migration was larger than that of water. In spite of these results, few studies have explored the difference between isothermal and non-isothermal models when assessing groundwater recharge taking account of the water table (Han et al. 2014).

The main goal of this study was to provide a more process-based ascertainment of the effects of soil temperature on groundwater recharge in arid and semi-arid regions. A lysimeter was adopted to accurately observe the amount of groundwater recharge in arid and semi-arid regions from 1 June to 30 September 2018. Subsequently, non-isothermal and isothermal models based on HYDRUS-1D software were developed. Observed soil moisture and soil temperature data were employed to calibrate both numerical models. The calibrated numerical models were then utilized to calculate the groundwater recharge. Based on the numerical results, a determination was made whether the effect of soil temperature can be overlooked when assessing groundwater recharge in arid and semi-arid regions.

Materials and methods

Study site

The lysimeter data applied here were obtained from in-situ experiments performed on the Ordos Plateau, northwestern China (Fig. 1). This study used a large non-weighing lysimeter with an initial water-table depth of 2.0 m below the surface. The lysimeter had a diameter of 2.0 m. To prevent water leakage, the bottom of the lysimeter was sealed. The lysimeter

Fig. 1 **a**–**b** Location of the Henan Town national weather station in China, and **c** photograph of a lysimeter outcrop

was filled with uniform sandy loam. The volumetric soil moisture content and soil temperature were monitored with ECH2O-5TM probes (Decagon Devices, Inc.), featuring an accuracy of approximately ±2%, installed in the lysimeter at various depths (3, 10, 20, 30, 50, 80, 150, 190, and 250 cm). Water-table fluctuations were observed with a CTD-Diver sensor (DI271, Van Essen, Inc.), featuring an accuracy of ±0.1%, installed deep in the lysimeter. The data were harvested at intervals of 5 min. Rainfall, wind speed, air temperature, and net radiation (i.e., the meteorological variables) were measured at intervals of 1 h. Soil samples were taken, and their soil-moisture retention curves were plotted in the laboratory using a Ku-pF apparatus (UGT GmbH, Muncheberg, Germany). The van Genuchten (1980) model was adopted to fit the soil-moisture retention curves. The experimental period lasted from 1 June to 30 September 2018.

The climate at the in situ experiment location is semi-arid, temperate, continental monsoon, exhibiting mean annual rainfall, potential evapotranspiration, and air temperature of 320 mm, 2,266 mm, and 8.0 °C, respectively (Zhang et al. 2018). Most of the annual rainfall (60–80%) occurs during the summer, from June to September. The in situ experiment location has been used for studies of the hydrological cycle on the Ordos Plateau since 2003. Based on previous studies, the main water exchange in arid and semi-arid regions occurs in the vertical direction (Chen et al. 2018); thus, a 1D numerical model was adopted to simulate water flow in this study.

Isothermal flow model

One-dimensional water movement in a partially saturated porous medium can be expressed by Richards' equation, in accordance with the assumptions that water flow resulting from thermal gradients can be overlooked:

$$\frac{\partial \theta}{\partial t} = \frac{\partial}{\partial z}\left[K(h)\left(\frac{\partial h}{\partial z} + 1\right)\right] \tag{1}$$

where θ denotes the volumetric water content (cm^3/cm^3); z is the vertical distance from the datum, with positive defined as upward (cm); t represents the time (T); $K(h)$ is the unsaturated hydraulic conductivity function (cm/T); and h refers to the pressure head (cm).

Non-isothermal flow model

A numerical HYDRUS-1D model (Simunek et al. 2013) was employed in this study to simulate both the vertical dual-phase flow and heat transport. The governing equation for the dual-phase flow is (Saito et al. 2006):

$$\frac{\partial \theta_T(h)}{\partial t} = \frac{\partial}{\partial z}\left[(K(h) + K_{vh})\left(\frac{\partial h}{\partial z} + 1\right) + (K_{LT} + K_{vT})\frac{\partial T}{\partial z}\right] \tag{2}$$

where θ_T is the total volumetric water content ($= \theta_L + \theta_v$) (cm^3/cm^3); θ_L denotes the volumetric liquid water content (cm^3/cm^3); θ_v is the volumetric water vapor content (cm^3/cm^3); t is the time (T); z is the vertical distance from the datum, with positive defined as upward (cm); h refers to the pressure head (cm); T is the soil temperature (°C); K_{vh} is the isothermal vapor hydraulic conductivity (cm/T); and K_{LT} (cm^2/°C/h) and K_{vT} (cm^2/°C/h) are the thermal hydraulic conductivity of the liquid phase and the thermal hydraulic conductivity of the vapor phase, respectively.

$K(h)$ and θ_L denote the nonlinear functions of h (van Genuchten 1980).

$$\theta(h) = \begin{cases} \theta_r + \dfrac{\theta_s - \theta_r}{[1 + |\alpha h|^n]^m} & h < 0 \\ \theta_s & h \geq 0 \end{cases} \tag{3}$$

$$K(h) = K_s S_e^l \left[1 - \left(1 - S_e^{1/m}\right)^m\right]^2 \tag{4}$$

where $S_e = \frac{\theta - \theta_r}{\theta_s - \theta_r}$, in which θ_r is the residual moisture content (cm^3/cm^3); θ_s is the saturated moisture content (cm^3/cm^3); α is a soil pore-size distribution parameter (1/cm); n is a function of the pore size distribution (–); and K_s is the saturated hydraulic conductivity of the soil (cm/T). K_{LT} is a function of K_{Lh}, h, and T, as computed internally with HYDRUS.

The heat transport is solved simultaneously to characterize the temperature distribution of the vertical profile. The equation governing heat transport, accounting for the effects of water vapor diffusion, is expressed as (Saito et al. 2006):

$$C_p(\theta_L)\frac{\partial T}{\partial t} + L_o\frac{\partial \theta_v}{\partial t}$$
$$= \frac{\partial}{\partial z}\left(\lambda(\theta_L)\frac{\partial T}{\partial z}\right) - C_w q_L \frac{\partial T}{\partial z} - C_v \frac{\partial(q_v T)}{\partial z} - L_o \frac{\partial q_v}{\partial z} \tag{5}$$

where $C_p(\theta_L)$, C_w, and C_v denote the volumetric heat capacity (J/cm^3/°C) of the porous medium, liquid water, and water vapor, respectively; L_o represents the volumetric latent heat of vaporization of liquid water (J/cm^3), computed internally as a function of air temperature; and $\lambda(\theta_L)$ is the thermal conductivity of the porous medium (J/°C/cm/h). $C_p(\theta_L)$ is determined by the time-varying θ_L and calculated internally.

The thermal conductivity $\lambda(\theta_L)$ is (de Marsily 1986):

$$\lambda(\theta_L) = \lambda_0(\theta_L) + \beta_T C_w |q| \tag{6}$$

where β_T denotes the thermal dispersity (5 cm); and $\lambda_0(\theta_L)$ is the baseline thermal conductivity, which is defined as (Chung and Horton 1987):

$$\lambda_0 = b_1 + b_2\theta_L + b_3\theta_L^{0.5} \tag{7}$$

where b_1, b_2, and b_3 represent empirical parameters (W/cm/°C). These parameters were based on the literature (Huang et al. 2016).

Initial and boundary conditions

Proper initial conditions are required to correctly simulate dual-phase flow and heat transport. For dual-phase flow, either the pressure head or the moisture content can act as the initial condition. In the respective model, this study linearly interpolated the moisture content measured at various depths on 1 June 2018 over the entire profile; the interpolated moisture content distribution acted as the dual-phase flow initial condition. Likewise, the soil temperature measured on 1 June 2018 was linearly interpolated over the entire profile, and the temperature distribution acted as the initial condition for the heat transport.

In each model, the top boundary was specified with an atmospheric boundary condition consisting of several time-dependent variables (e.g., net radiation, precipitation, air temperature, relative humidity, and wind speed). These time-dependent variables were adopted to calculate the evaporation rates and ground heat fluxes required as direct boundary conditions to solve the governing equations for dual-phase flow and heat transport. Time-dependent pressure head and temperature variables were assigned to the bottom boundary of each model in order to simulate the dual-phase flow and heat transport, respectively.

The models were split into two layers for the lysimeter using correlation analysis of the moisture content time series. The single layers in both models were initially tested after the lysimeter had been packed with identical sandy loam soil (Zhang et al. 2018), although reasonable fitting statistics could not be calculated for soil moisture and soil temperature simultaneously. Thus, two layers were adopted based on correlation analysis. The soil heterogeneity most likely resulted from uneven packing and later salt movement driven by evaporation (Hernández-López et al. 2016). More layers could be exploited to enhance the model's accuracy, although this would obviously increase the number of uncertain parameters requiring calibration. Thus, the number of layers complied with a compromise between accuracy and the degree of freedom of the model.

Model parameters were required for all of the layers. Given the number of layers considered, the measured soil hydraulic parameters acted as initial estimates of the parameter values. All of the parameters were derived from the following calibration process:

$$\text{Bias} = \frac{1}{N} \sum_{n=1}^{N} (\theta_{\text{sim}} - \theta_{\text{obs}}) \tag{8}$$

$$\text{RMSE} = \sqrt{\frac{1}{N} \sum_{n=1}^{N} (\theta_{\text{sim}} - \theta_{\text{obs}})^2} \tag{9}$$

where n denotes the number of days; and θ_{sim} and θ_{obs} refer to the simulated and observed values of a variable on the ith day, respectively. Since both the soil moisture and temperature acted as calibration targets, a total of four metrics were assessed for the respective model. The calibration module included in HYDRUS-1D was employed here to optimize $\theta_{\text{s}}, \theta_{\text{r}}, \alpha,$ and n for all of the layers (Table 1).

Results

Rainfall and groundwater level

Rainfall data for the study area were collected from 2014 to 2018. The mean annual rainfall for this area was 315.9 mm, approximately 80% of which occurred between June and September. Most of the rainfall events were light, with the majority <5 mm. The frequency decreased as the amount of the individual rainfall events increased from 5 to 50 mm. Light rainfall events (< 5.0 mm) were most frequent, whereas larger rainfall events (≥10.0 mm) were infrequent but considerably impacted the total rainfall. The percentages of the total amount and frequency of events decreased with increasing rainfall. All of these characteristics exhibited the rainfall pulse patterns of a semi-arid area. Figure 2 presents the fluctuations in water table depth and precipitation at the study location for the experiment period. A total of 34 rainfall events occurred during the experimental period. The maximum and minimum amounts of rainfall were 4.35 and 0.01 cm, respectively, and 73% percent of the rainfall events were <1 cm.
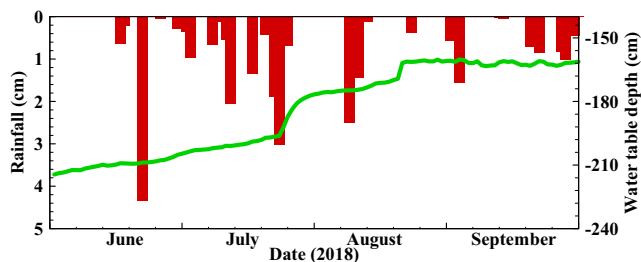
Moreover, the groundwater level fluctuations in the lysimeter were primarily affected by precipitation. The groundwater level always maintained an increasing trend, indicating that evaporation only slightly impacted groundwater. During the experiment, the groundwater level rose by 49.1 cm.

Soil moisture and temperature

The observed and calculated daily average soil temperatures at depths of 10 and 150 cm below the ground surface were simulated with the non-isothermal model (Fig. 3). The bias and RMSE at the depths of 10 and 150 cm were –0.27 and 2.7 °C and –0.8 and 1.1 °C, respectively. Figure 3a,b shows that the calculated soil temperature was fitted at the observed depths, demonstrating that the non-isothermal model could be exploited to simulate heat transport in the vadose zone. Both the observed and simulated soil temperatures exhibited diurnal periodic patterns, as imposed by the underlying soil

Table 1 Calibrated parameters of the van Genuchten model

Layer	θ_{s} (cm³/cm³)	θ_{r} (cm³/cm³)	α (cm⁻¹)	n
Layer 1 (0–7 cm)	0.31	0.01	0.02	2.03
Layer 2 (7—250 cm)	0.34	0.01	0.043	1.61

Fig. 2 Distribution of rainfall (red bars) and variation in water table depth (green line) during the experimental period

temperature wave at the water table and the overlying atmospheric conditions. The soil temperature close to the upper boundary fluctuated more significantly; for instance, the average diurnal amplitude of the soil temperature at a depth of 3 cm was approximately 30 °C (not shown in Fig. 3). As the depth increased, the amplitude and delay decreased; for instance, the average diurnal amplitude of the soil temperature at a depth of 150 cm was <1 °C. In addition, rainfall events could also affect the amplitude of the soil temperature as a result of less net radiation and lower air temperatures.

The measured soil moisture content and the values simulated with the non-isothermal model at depths of 10 and 150 cm are presented in Fig. 3c,d. As suggested from the figures, the measured and simulated soil moisture content values typically fluctuated due to rainfall events, especially in the upper soil layers (e.g., at a depth of 10 cm). Yeh and Eltahir (2005) pointed out that groundwater and soil moisture act as two low-pass filters of atmospheric forcing, thereby causing the fluctuation amplitudes

to attenuate with depth. Accordingly, the amplitude of the soil moisture at a depth of 150 cm was <0.01 cm/cm. The non-isothermal model, which considers liquid water and heat transport, effectively captured the sharp increase in the soil-moisture content and the general decrease with depth. The bias and RMSE at depths of 10 and 150 cm were −0.0009 and 0.016 (cm^3/cm^3) and 0.00035 and 0.016 (cm^3/cm^3), respectively. It was therefore revealed that the non-isothermal model could be used to assess groundwater recharge.

The simulated results of the isothermal model at depths of 10 and 150 cm are illustrated in Fig. 4. As indicated by the figure, the isothermal model slightly underestimated near-surface soil moisture. The bias and RMSE values at 10 and 150 cm reached −0.0088 and 0.018 (cm^3/cm^3) and −0.002 and 0.016 (cm^3/cm^3), respectively, demonstrating that the isothermal model could reproduce the observed soil-moisture data.

Cumulative evaporation

Evaporation is critical to the hydrological cycle, representing a water flux interaction between the ground surface and the atmosphere. Figure 5 illustrates the observed cumulative evaporation and the values estimated with the non-isothermal and isothermal models. At the end of the experiment, the cumulative evaporation values reached 20.13, 20.90, and 23.40 cm for the observations, the non-isothermal model, and the isothermal model, respectively. The non-isothermal model results comply with the observed results, whereas the isothermal model overestimated the
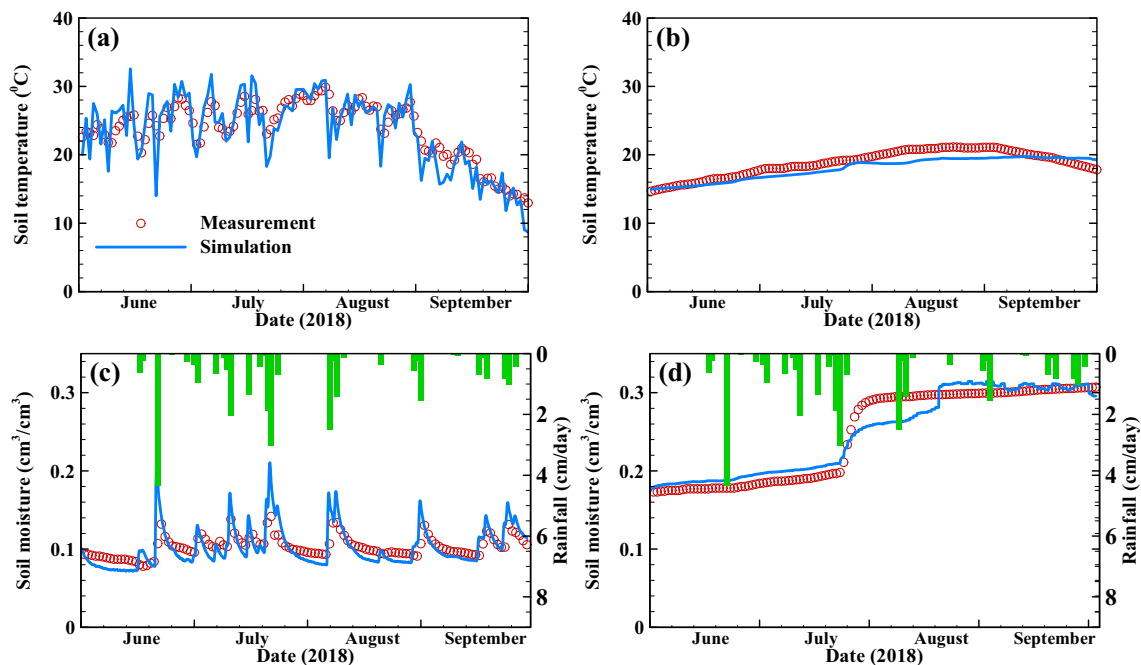
Fig. 3 Variations in the observed soil temperature (circles) at depths of **a** 10 cm and **b** 150 cm, and soil moisture (circles) at depths of **c** 10 cm and **d** 150 cm. The blue lines represent the values calculated with the non-isothermal model and the green bars denote rainfall events
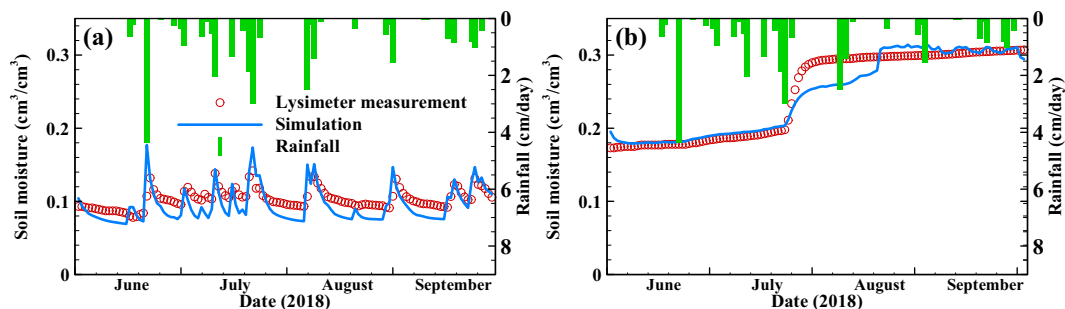
Fig. 4 Variations in the observed soil moisture (red circles) at depths of **a** 10 cm and **b** 150 cm. The blue lines represent the values calculated with the isothermal model

values by 16.2%. Figure 5 indicates that the cumulative evaporation values calculated with the 2 models were similar in mid-June. After the rainfall events in late June, the results of the models progressively diverged with time. The cumulative evaporation assessed with the non-isothermal model continuously increased in response to precipitation, while the isothermal model significantly overestimated the evaporation values in the experiment. It was therefore demonstrated that the non-isothermal model is more applicable to the calculation of evaporation during rainy periods than the isothermal model.
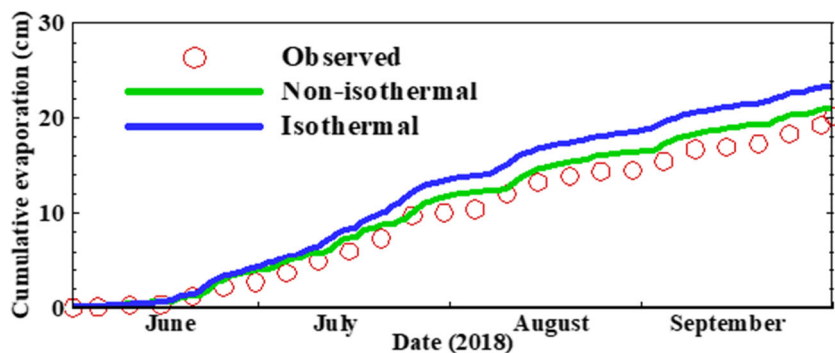
Cumulative groundwater recharge

The cumulative groundwater recharge ascertained from the lysimeter observations as well as the non-isothermal and iso-thermal models are illustrated in Fig. 6. At the end of the experiment, the cumulative groundwater recharge reached 8.30, 8.33, and 7.24 cm for the observed results, the non-isothermal model, and the isothermal model, respectively. Thus, the isothermal model underestimated the cumulative groundwater recharge by 13.2%. The observed and simulated results all increased slightly from June to mid-July. In response to heavy rainfall events, the amount of recharge significantly increased by 2.6 cm from August 19 to August 29. The distribution of the cumulative groundwater recharge values calculated with the non-isothermal model complied with the levels of the measured data were more closely than the values calculated with the isothermal model. The

differences between the values simulated with the non-isothermal and isothermal models increased continuously over time after June. The isothermal model led to the under-estimation of recharge, especially after heavy rainfall. As demonstrated by these results, the non-isothermal model more accurately estimates groundwater recharge under natural conditions.

Discussion

Rainfall infiltration critically impacts groundwater recharge. Insights into the mechanism of groundwater recharge should also be gained in order to assist groundwater-water-resource management. Accurately assessing groundwater recharge is challenging, due to the difficulty of obtaining field observations, numerous controlling factors, and complex physical mechanisms (Chen et al. 2012). According to the results of this study, the non-isothermal model can produce more accurate groundwater recharge results, indicating that the non-isothermal model outperforms the isothermal model in simulating evaporation, which overlooks the thermal and vapor fluxes. The smaller groundwater recharge values produced by the isothermal model may also stem from its over-estimation of evaporation during rainfall events. The variations in the evaporation of both models during rainfall events were plotted (Fig. 7a). As can be seen in this figure, the isothermal model underestimated evaporation after the

Fig. 5 Temporal variations in the cumulative evaporation from the lysimeter observations (circles) and calculated with the non-isothermal (green line) and iso-thermal (blue line) models during the experimental period

Fig. 6 Temporal variations in the cumulative groundwater recharge from the lysimeter observations (green squares) and calculated with the non-isothermal (blue dotted line) and isothermal (black dotted line) models during the experimental period
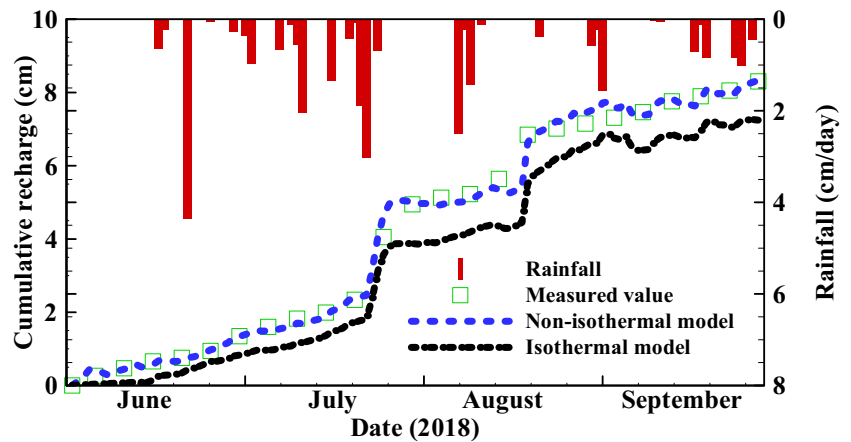
precipitation ended (e.g., from July 23–25). In contrast, the isothermal model overestimated evaporation during dry periods (e.g., from July 25–August 7; Fig. 7a). These factors caused the cumulative evaporation calculated with the isothermal model to be greater than that of the non-isothermal model (Fig. 5).

The accuracy of the estimated evaporation affected the groundwater recharge calculations. According to Fig. 7b, the groundwater recharge values estimated with the non-isothermal and isothermal models rose by 0.87 and 0.69 cm, respectively, during the heavy rainfall events from July 20–August 6. Furthermore, the water flux near the surface after

Fig. 7 Temporal variations in **a** evaporation, **b** cumulative groundwater recharge, and **c** water flux near the surface on 26 July, calculated with the non-isothermal (red line) and isothermal (green line) models
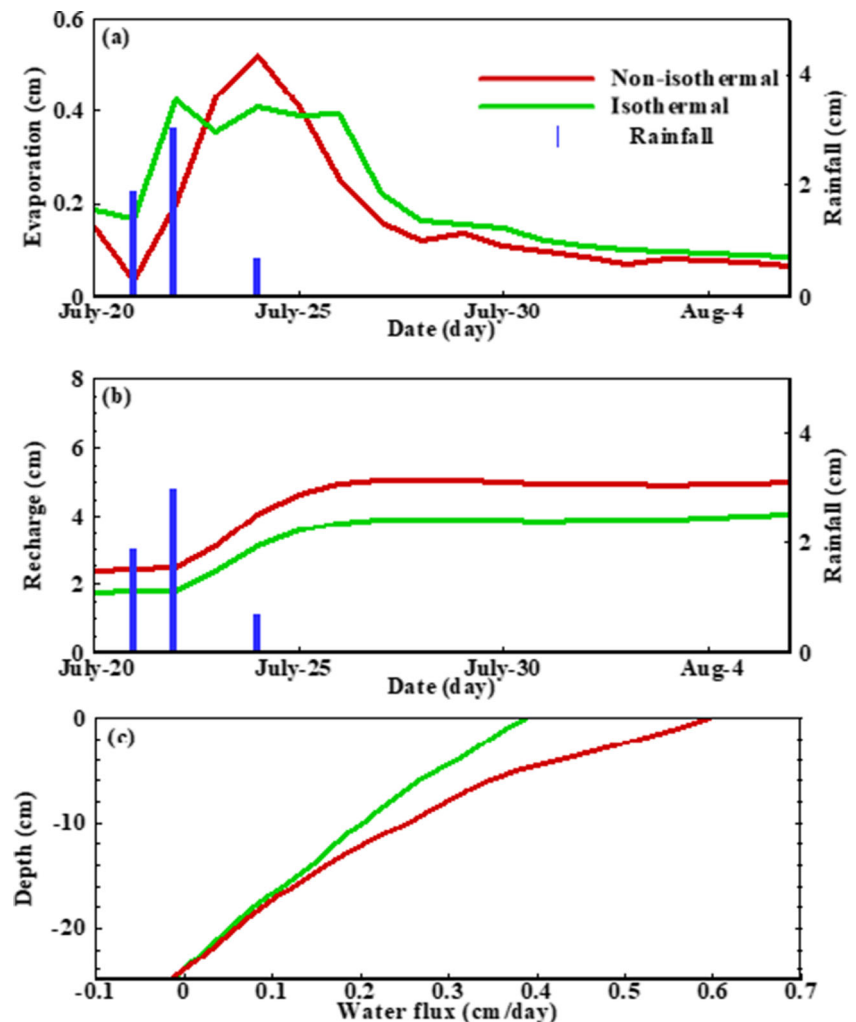
the rainfall event on August 24 was plotted (see Fig. 7c). The water flux value produced with the isothermal model was significantly less prominent than that produced with the non-isothermal model. As revealed from these results, the isothermal model overestimated evaporation, thereby yielding a low value for infiltration water flux. Ultimately, the groundwater recharge was underestimated with the isothermal model.

Conclusions

In the present study, a lysimeter was adopted to collect data in the Mu Us Desert, located in the Ordos Basin of China. Subsequently, these measurements were utilized to assess the groundwater recharge results of non-isothermal and isothermal numerical models. These models were developed to simulate evaporation and groundwater recharge. Both models were calibrated based on lysimeter data for 122 summer days. The observed soil hydraulic properties were employed to parameterize the model. The models were driven by meteorological forcing data (e.g., net radiation, wind speed, and air temperature). The soil moisture and temperature observations, along with the soil profile, were used to calibrate the model. The simulated soil moisture and temperature results were found to be consistent with the observed values, demonstrating that both models can satisfactorily simulate these parameters. Compared to the isothermal model, the non-isothermal model could more accurately assess the evaporation and groundwater recharge. The isothermal model overestimated evaporation by 16.2%, while underestimating groundwater recharge by 13.2%. The isothermal model overestimated evaporation in dry periods, thereby causing the infiltration flux to be underestimated.

The lysimeter observations were useful since they allowed for exploration of the differences between the isothermal and non-isothermal numerical models. Given the implications of soil temperature in the simulation of groundwater recharge in arid and semi-arid regions, the non-isothermal model is considered as a better choice. Due to the complexity of the non-isothermal model, however, comprehensive uncertainty analysis is required. The results presented here are important as they provide additional insight into the groundwater recharge processes taking account of the water table.

References

Batalha MS, Barbosa MC, Faybishenko B, Van Genuchten MT (2018) Effect of temporal averaging of meteorological data on predictions of groundwater recharge. J Hydrol Hydromech 66(2):143–152

Bhaskar AS, Hogan DM, Nimmo JR, Perkins KS (2018) Groundwater recharge amidst focused stormwater infiltration. Hydrol Process 32(13):2058–2068

Bergström L (1990) Use of lysimeters to estimate leaching of pesticides in agricultural soils. Environ Pollut 67(4):325–347

Camacho Suarez VV, Saraiva Okello AML, Wenninger JW, Uhlenbrook S (2015) Understanding runoff processes in a semi-arid environment through isotope and hydrochemical hydrograph separations. Hydrol Earth Syst Sci 19(10):4183–4199

Chen X, Huang Y, Ling M, Hu Q, Liu B (2012) Numerical modeling groundwater recharge and its implication in water cycles of two interdunal valleys in the Sand Hills of Nebraska. Phys Chem Earth Parts A/B/C 53:10–18

Chen L, Wang W, Zhang Z, Wang Z, Wang Q, Zhao M, Gong C (2018) Estimation of bare soil evaporation for different depths of water table in the wind-blown sand area of the Ordos Basin, China. Hydrogeol J 26(5):1693–1704

Chung S-O, Horton R (1987) Soil heat and water flow with a partial surface mulch. Water Resour Res 23(12):2175–2186

Cuthbert MO, Acworth RI, Andersen MS, Larsen JR, McCallum AM, Rau GC, Tellam JH (2016) Understanding and quantifying focused, indirect groundwater recharge from ephemeral streams using water table fluctuations. Water Resour Res 52(2):827–840

de Marsily G (1986) Quantitative hydrogeology. Academic Press, London

Gleeson T, Befus KM, Jasechko S, Luijendijk E, Cardenas MB (2016) The global volume and distribution of modern groundwater. Nat Geosci 9(2):161–167

Gosselin JS, Rivard C, Martel R, Lefebvre R (2016) Application limits of the interpretation of near-surface temperature time series to assess groundwater recharge. J Hydrol 538:96–108

Han J, Zhou Z, Fu Z, Wang J (2014) Evaluating the impact of nonisothermal flow on vadose zone processes in presence of a water table. Soil Sci 179(2):57–67

Hartmann A, Gleeson T, Wada Y, Wagener T (2017) Enhanced groundwater recharge rates and altered recharge sensitivity to climate variability through subsurface heterogeneity. Proc Natl Acad Sci 114(11):2842–2847

Hamed Y (2013) The hydrogeochemical characterization of groundwater in Gafsa-Sidi Boubaker region (southwestern Tunisia). Arab J Geosci 6(3):697–710

Hernández-López MF, Braud I, Gironás J, Suárez F, Muñoz JF (2016) Modelling evaporation processes in soils from the Huasco salt flat basin, Chile. Hydrol Process 30(25):4704–4719

Huang J, Hou R, Yang H (2016) Diurnal pattern of liquid water and water vapor movement affected by rainfall in a desert soil with a high water table. Environ Earth Sci 75(1):73

Huang T, Pang Z, Liu J, Ma J, Gates J (2017) Groundwater recharge mechanism in an integrated tableland of the loess plateau, northern China: insights from environmental tracers. Hydrogeol J 25(7):2049–2065

Hou L, Wang XS, Hu BX, Shang J, Wan L (2016) Experimental and numerical investigations of soil water balance at the hinterland of the Badain Jaran Desert for groundwater recharge estimation. J Hydrol 540:386–396

Jin G, Shimizu Y, Onodera S, Saito M, Matsumori K (2015) Evaluation of drought impact on groundwater recharge rate using SWAT and Hydrus models on an agricultural island in western Japan. Proc Int Assoc Hydrol Sci 371:143

Li Z, Chen X, Liu W, Si B (2017) Determination of groundwater recharge mechanism in the deep loessial unsaturated zone by environmental tracers. Sci Total Environ 586:827–835

Lu X, Jin M, van Genuchten MT, Wang B (2011) Groundwater recharge at five representative sites in the Hebei plain, China. Groundwater 49(2):286–294

Meixner T, Manning AH, Stonestrom DA, Allen DM, Ajami H, Blasch KW, Brookfield AE, Castro CL, Clark JF, Gochis DJ, Flint AL, Neff KL, Niraula R, Rodell M, Scanlon BR, Walvoord MA (2016) Implications of projected climate change for groundwater recharge in the western United States. J Hydrol 534:124–138

Meshkat M, Warner RC, Walton LR (1999) Lysimeter design, construction, and instrumentation for assessing evaporation from a large undisturbed soil monolith. Appl Eng Agric 15(4):303

Meissner R, Rupp H, Seeger J, Ollesch G, Gee GW (2010) A comparison of water flux measurements: passive wick-samplers versus drainage lysimeters. Eur J Soil Sci 61(4):609–621

Moeck C, Radny D, Auckenthaler A, Berg M, Hollender J, Schirmer M (2017) Estimating the spatial distribution of artificial groundwater recharge using multiple tracers. Isot Environ Health Stud 53(5):484–499

Nimmo JR, Horowitz C, Mitchell L (2015) Discrete-storm water-table fluctuation method to estimate episodic recharge. Groundwater 53(2):282–292

Purandara BK, Venkatesh B, Jose MK, Chandramohan T (2018) Change of land use/land cover on groundwater recharge in Malaprabha catchment, Belagavi, Karnataka, India. In: Groundwater. Springer, Singapore, pp 109–120

Ren R, Ma J, Cheng Q, Zheng L, Guo X, Sun X (2017a) Modeling coupled water and heat transport in the root zone of winter wheat under non-isothermal conditions. Water 9(4):290

Ren R, Ma J, Cheng Q, Zheng L, Guo X, Sun X (2017b) An investigation into the effects of temperature gradient on the soil water–salt transfer with evaporation. Water 9(7):456

Saito H, Šimůnek J, Mohanty BP (2006) Numerical analysis of coupled water, vapor, and heat transport in the vadose zone. Vadose Zone J 5(2):784–800

Sakram G, Adimalla N (2018) Hydrogeochemical characterization and assessment of water suitability for drinking and irrigation in crystalline rocks of Mothkur region, Telangana state, South India. Appl Water Sci 8(5):143

Simunek JJ, Šejna M, Saito H, Sakai M, Van Genuchten M (2013) The hydrus-1D software package for simulating the movement of water, heat, and multiple solutes in variably saturated media, version 4.17. HYDRUS software series 3, Department of Environmental Sciences, University of California Riverside, Riverside, California

Szymkiewicz A, Tisler W, Burzyński K (2015) Examples of numerical simulations of two-dimensional unsaturated flow with VS2DI code using different interblock conductivity averaging schemes. Geologos 21(3):161–167

Tonkul S, Baba A, Şimşek C, Durukan S, Demirkesen AC, Tayfur G (2019) Groundwater recharge estimation using HYDRUS 1D model in Alaşehir sub-basin of Gediz Basin in Turkey. Environ Monit Assess 191(10):610

Turkeltaub T, Kurtzman D, Bel G, Dahan O (2015) Examination of groundwater recharge with a calibrated/validated flow model of the deep vadose zone. J Hydrol 522:618–627

van Genuchten MTh (1980) A closed-form equation for predicting the hydraulic conductivity of unsaturated soils. Soil Sci Soc Am J 44(5):892–898

Varis O (2014) Resources: curb vast water use in Central Asia. Nature News 514(7520):27

Wang W, Zhao G, Li J, Hou L, Li Y, Yang F (2011) Experimental and numerical study of coupled flow and heat transport. In: Proceedings of the Institution of Civil Engineers-Water Management, vol 164, no. 10. Thomas, London, pp 533–547

Xu Y, Beekman HE (2019) Groundwater recharge estimation in arid and semi-arid southern Africa. Hydrogeol J 27(3):929–943

Yeh PJ-F, Eltahir EAB (2005) Representation of water table dynamics in a land surface scheme. Part I: model development. J Clim 18(12):1861–1880

Zhang Z, Wang W, Wang Z, Chen L, Gong C (2018) Evaporation from bare ground with different water-table depths based on an in-situ experiment in Ordos plateau, China. Hydrogeol J 26(5):1683–1691

Zhao K, Jiang X, Wang X, Wan L (2020) Restriction of groundwater recharge and evapotranspiration due to a fluctuating water table: a study in the Ordos Plateau, China. Hydrogeol J. https://doi.org/10.1007/s10040-020-02208-9